Carbohydrate Polymers 112 (2014) 165–172

Contents lists available at ScienceDirect

Carbohydrate Polymers

journal homepage: www.elsevier.com/locate/carbpol

Improvement of polyvinyl alcohol properties by adding nanocrystalline cellulose isolated from banana pseudostems

André Luís S. Pereira[a], Diego M. do Nascimento[b], Men de sá M. Souza Filho[c], João Paulo S. Morais[d], Niedja F. Vasconcelos[b], Judith P.A. Feitosa[b], Ana Iraidy S. Brígida[e], Morsyleide de F. Rosa[c,*]

[a] Universidade Federal do Ceará (UFC), Centro de Tecnologia, Campus do Pici, Engenharia e Ciência dos Materiais, Bloco 714, CEP 60455-900 Fortaleza, Ceará, Brazil
[b] Universidade Federal do Ceará (UFC), Centro de Ciências, Campus do Pici, Departamento de Química Orgânica e Inorgânica, Bloco 940, CEP 60455-760 Fortaleza, Ceará, Brazil
[c] Embrapa Agroindústria Tropical – CNPAT, Rua Dra Sara Mesquita 2270, Planalto do Pici, CEP 60511-110 Fortaleza, Ceará, Brazil
[d] Embrapa Algodão – CNPA, Rua Oswaldo Cruz 1143, Centenário, CEP 58428-095 Campina Grande, Paraíba, Brazil
[e] Embrapa Agroindústria de Alimentos, Av. das Américas, 29501, CEP 23020-470 Rio de Janeiro, RJ, Brazil

ARTICLE INFO

Article history:
Received 6 March 2014
Received in revised form 2 May 2014
Accepted 19 May 2014
Available online 6 June 2014

Keywords:
Packaging
Nanotechnology
Agribusiness
Musa sp.
Casting
Nanocrystals

ABSTRACT

Cellulose nanocrystals (CNCs) isolated from banana pseudostems fibers (BPF) of the Pacovan variety were used as fillers in a polyvinyl alcohol (PVOH) matrix to yield a nanocomposite. The fibers from the external fractions of the BPF were alkaline bleached and hydrolyzed under acidic conditions (H_2SO_4 62% w/w, 70 min, 45 °C) to obtain CNCs with a length (L) of 135.0 ± 12.0 nm and a diameter (D) of 7.2 ± 1.9 nm to yield an aspect ratio (L/D) of 21.2. The CNCs were applied to PVOH films at different concentrations (0%, 1%, 3%, and 5% w/w, dry basis). With higher concentrations of CNCs, the water–vapor barrier of the films increased, while the optical properties changed very little. Increasing the concentration of the CNCs up to 3% significantly improved the mechanical properties of the nanocomposite.

1. Introduction

Cellulose is a carbohydrate polymer and the most abundant natural biodegradable macromolecule in plants. It is the main structural constituent of plant fibers and provides mechanical strength and stability. To obtain cellulose from lignocellulosic sources, different processes can be applied to remove components surrounding the crystalline cellulosic nanofibers. These treatments allow for the generation of materials with high crystallinity and large surface areas, which are desirable characteristics for generating products on the nanometer scale (Abdul Khalil, Bhat, & Ireana Yusra, 2012; Dufresne, 2012; Elanthikkal, Gopalakrishnapanicker, Varghese, & Guthrie, 2010; Faruk, Bledzkia, Fink, & Sain, 2012).

The use of cellulose in polymer production has attracted attention because of its wide applicability in products such as biocomposites and nanocomposites. Cellulose nanocomposites exhibit exceptional properties making nanofibers one of the most attractive classes of materials for making nanocomposites (Moon, Martini, Nairn, Simonsen, & Youngblood, 2011).

Two types of nanocellulose can be obtained from cellulose: whiskers and nanofibrils (AziziSamir, Alloin, & Dufresne, 2005). The term “whiskers” (or “nanowhiskers/nanocrystals”) is used to refer to nanoparticles that exhibit a needle-like appearance, while the term “nanofibrils” (or “microfibrillated cellulose”) is used to designate long and flexible nanoparticles composed of alternating amorphous and crystalline domains (Abdul Khalil et al., 2012).

Different approaches have been employed to prepare nanocellulose in the form of either nanofibrils or nanocrystals. In general, “top-down” nanoscale structures are obtained by the size reduction or deconstruction of cellulosic materials (Yousefi et al., 2013) such as wood, plant fibers, and agricultural residues such as banana

* Corresponding author. Tel.: +55 85 3391 7344; fax: +55 85 3391 7109.
E-mail addresses: andre110487@gmail.com (A.L.S. Pereira), diego@alu.ufc.br (D.M.d. Nascimento), men.souza@embrapa.br (M.d.s.M. Souza Filho), joao.morais@embrapa.br (J.P.S. Morais), niedjafittipaldi@hotmail.com (N.F. Vasconcelos), judith@dqoi.ufc.br (J.P.A. Feitosa), ana.iraidy@embrapa.br (A.I.S. Brígida), morsyleide.rosa@embrapa.br, morsyleide@gmail.com (M.d.F. Rosa).

http://dx.doi.org/10.1016/j.carbpol.2014.05.090
0144-8617/

pseudostems. However, variations in the sources and conditions under which cellulosic materials are prepared may lead to a wide range of structures with different properties and applications that ultimately affect the performance of the final product (Azeredo, Miranda, Rosa, Nascimento, & Moura, 2012; Dufresne, 2012; Jiang, Liu, Zhang, Wang, & Wang, 2007; Kvien & Oksman, 2007).

The amorphous regions of cellulose can be broken under controlled conditions to liberate colloidal particles known as cellulose nanocrystals (CNCs). This is achieved by acid hydrolysis, which entails the destruction of the surrounding amorphous regions between the microfibrils of cellulose, while the crystalline segments remain intact. This breakdown of CNCs is attributed to the fact that the kinetics of hydrolysis is faster in the amorphous region than in the crystalline domains because of the higher permeability of the former (Azizi Samir et al., 2005). The geometric dimensions depend on the initial source of cellulose, which accounts for widths between 5 and 20 nm and lengths between 100 nm and 1–2 μm. In polar solvents (such as water and dimethylformamide), CNCs do not flocculate because of the electrostatic repulsion arising from the surface, leading to suspensions that are stable for several months (Tingaut, Zimmermann, & Sèbe, 2012).

Banana (*Musa* spp.) is a staple food grown in more than 120 countries in the world, with a production higher than 100 million tons in 2012, in a harvested area of almost 5 million hectares (FAOStat, 2014). The pseudostem is a high density and large scale crop biomass that is usually disposed of after the fruit has been harvested, what can yield ≈1 billion tons of wasted banana biomass (FAOStat, 2014; Padam, Tin, Chye, & Abdullah, 2012), which may spread diseases and pollute water sources (Santa-Maria, Ruiz-Colorado, Cruz, & Jeoh, 2013). However, this is an inexpensive and abundant source of carbohydrates, which remains mostly unexploited for biobased products manufacturing (Mueller, Weder, & Foster, 2014; Padam et al., 2012).

With the growing number of studies on lignocellulosic materials, there is a corresponding increase in the awareness of eco-friendly processes. Among the processes employed on the industrial scale, totally chlorine free (TFC) approaches are desirable in obtaining cellulose pulp, as they do not involve the use of chlorine and its derivatives that are known to pose environmental threats, especially when handled incorrectly. They also allow for the scale-up of a number of industrial processes, and thus lead to cost reductions (Khider, Omer, & Elzaki, 2012; Rosa, Rehman, Miranda, Nachtigall, & Bica, 2012).

Polyvinyl alcohol (PVOH) is among the biodegradable polymers that interact with nanocellulose and is a hydrophilic polymer that forms hydrogen bonds with nanocellulose. It has been studied as a polymeric matrix in the construction of nanocomposite films because of its versatility and wide spectrum of applications that can be improved by incorporating nanostructures (Chen, Lawton, Thompson, & Liu, 2012; Frone et al., 2011; Panaitescu et al., 2011; Rescignano et al., 2014; Roohani et al., 2008; Zhou, Fu, Zheng, & Zhan, 2012).

Here, we characterize the CNCs isolated from bleached banana pseudostem fibers (BPF) and evaluate the mechanical, permeability, and optical properties of PVOH nanocomposite films incorporated with CNCs, which can be applied in packaging materials.

2. Experimental

2.1. Plant materials and chemicals

Samples of *Musa sp.* (Pacovan variety) were harvested from a banana plantation in the experimental field of Embrapa Agroindústria Tropical (Paraipaba city, Ceará State, Brazil) in January 2011. The samples were obtained by cutting the pseudostems of randomly selected banana plants. The material was stored at 10 °C prior to separation and analysis.

The reagents used were of analytical grade (Vetec Quimica Fina Ltda, Duque de Caxias, RJ, Brazil) and included 97% (w/w) NaOH, 30% (w/w) H_2O_2, and 98% (w/w) H_2SO_4. The reagents were used as received without any additional purification. PVOH, type 40–88, was provided by Clariant S.A. (Vila Almeida, SP, Brazil).

2.2. Pretreatment of raw material – BPF

The BPF was blended in a FORTINOX cutting mill and pretreated as described in the literature with slight modifications (Borysiak & Doczekalska, 2005). Briefly, the bleaching process was performed by stirring 15.0 g of fiber in 10% (w/v) NaOH at 80 °C for 5 min in a ratio of 1:20 (g/mL). Then, 60 mL of 30% (v/v) H_2O_2 was added to the mixture and stirred for 30 min at 80 °C. After this step, the same volume of hydrogen peroxide was added to the solution, resulting in ≈420 mL of bleaching medium, which was stirred again for 30 min at 80 °C.

The fibers were filtered using a Buchner funnel and Whatman filter paper (23 μm pore size), and were washed with tap water until a pH close to neutrality was obtained. Then, the fibers were washed with distilled water, dried, and stored in a glass flask at 4 °C.

2.3. Isolation of CNCs

CNCs were isolated as described by Orts et al. (2005) and Rosa et al. (2010). Briefly, 4.0 g of bleached fiber was treated with 50.0 mL of 64% (w/w) sulfuric acid at 45 °C and stirred for 70 min. The reaction was stopped by adding 250 mL of cold deionized water (≈5 °C). The resulting suspension was then centrifuged (26,400 g, 15 min, 4 °C) and washed three times. Ultrasonic treatment (99 W for 3 min) was applied between each centrifugation step. At the end of the washing process, a cloudy supernatant was obtained and concentrated in a rotary evaporator (105 rpm, 57 °C, 40 mbar), yielding a gelatinous layer in the flask. The gel was dialyzed until a pH similar to the dialysis water (≈24 h) was obtained. Subsequently, the neutralized gel formed a stable colloidal suspension (≈1.8%, w/w) and was stored at 4 °C.

2.4. Preparation of composite films

A matrix suspension of polyvinyl alcohol (PVOH) was obtained by stirring PVOH granules (10%, w/w) in heated (80 °C) distilled water for 1 h. Calculated volumes of the PVOH solution were added to the CNC suspensions resulting in a final PVOH concentration of (6%, w/w) and CNC concentrations (dry wt. basis) of 1% (PVOH1), 3% (PVOH3), and 5% (PVOH5). The PVOH suspension was added to distilled water to prepare the neat film (PVOH0).

The films were casted in MYLAR laminar (commercial polyester film) adhered on glass plates (30 cm × 30 cm) and were adjusted to 1 mm spacing. The films were dried on a laboratory bench at ≈25 °C and a relative humidity of ≈74% for 24 h. After drying, the films were placed in a desiccator with a relative humidity of 55 ± 5% and a temperature of 25 ± 2 °C.

2.5. Characterization of materials

2.5.1. Chemical characterization

The moisture, extractive, and Klason lignin contents of BPF were determined in accordance to TAPPI T 421 om-02 (2002), TAPPI T 204 cm-97 (1997), and TAPPI T 222 om-22 (2000), respectively. The hemicellulose and alpha-cellulose contents were analyzed as

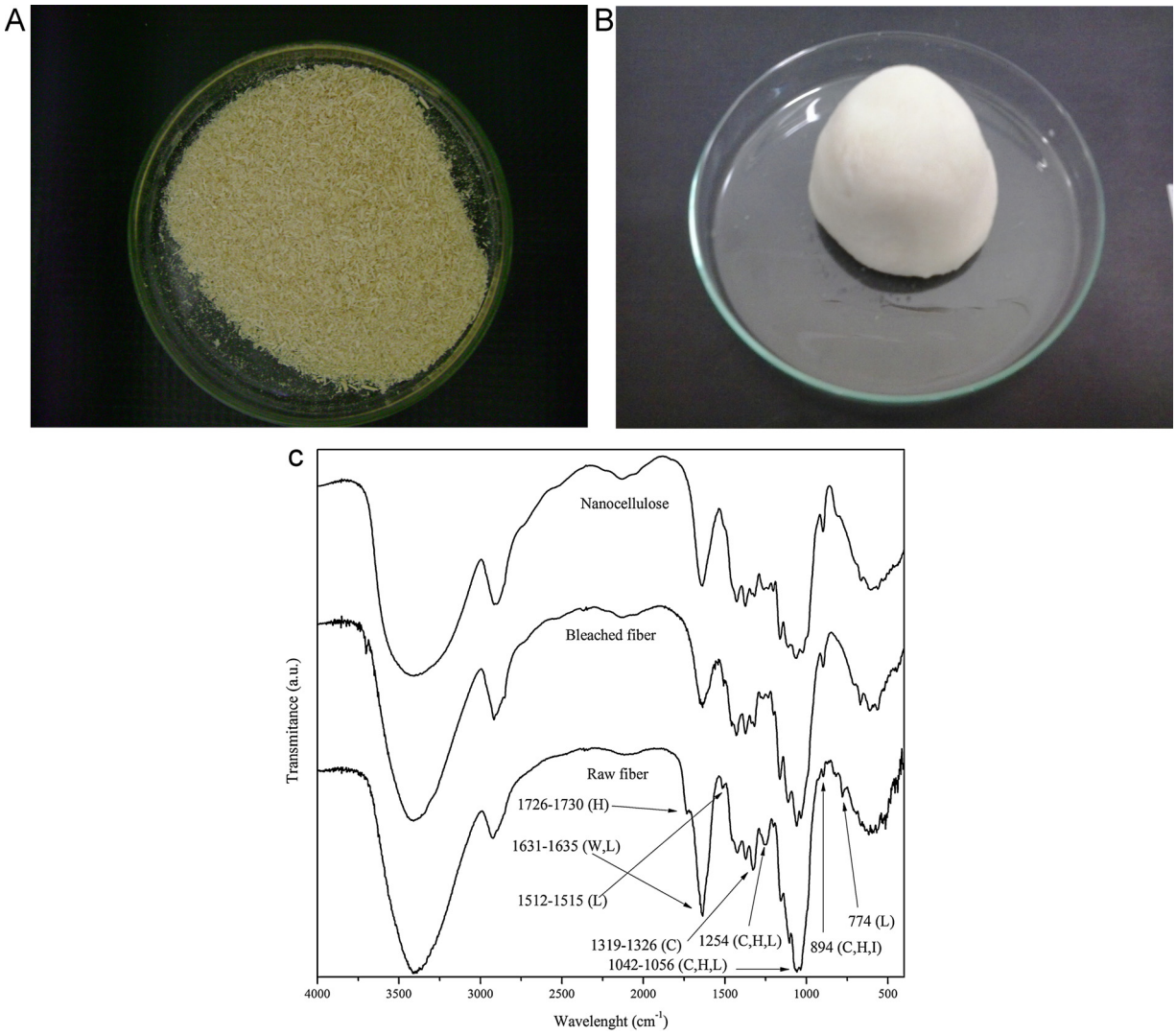

Fig. 1. Raw (a) and bleached (b) banana pseudostem fiber (BPF) and FTIR (c) spectra of raw (bottom) and bleached (middle) BPF, and nanocellulose (top).

described by Yokoyama, Kadla, & Chang (2002) and TAPPI T 203 cm-99 (2009).

2.5.2. FTIR

FTIR spectra were obtained in a Shimadzu FTIR-8300 spectrophotometer over a wavenumber interval of 4000–400 cm^{-1} at a 4 cm^{-1} resolution with 3% (w/w) KBr pellets.

2.5.3. Thermal analysis (TGA and DTG)

Thermogravimetric analysis (TGA) of ≈8 mg of each sample were performed in platinum crucibles using a Q50 Universal V20.10 (TA Instruments) thermal analyzer, from 25 °C to 700 °C with a heating rate of 10 °C/min, under a synthetic air atmosphere with a flux of 60 mL/min.

2.5.4. Differential scanning calorimetry (DSC)

DSC measurements were performed with ≈5.0 mg of plant material in sealed platinum crucibles and ≈2.3 mg of nanocomposite films in open platinum crucibles using a Universal V4.7a Q20 (TA Instruments) under a nitrogen atmosphere with a flux of 50 mL/min. The plant materials were heated over a temperature range 0–400 °C with a constant heating rate of 10 °C/min. The nanocomposite films were heated from −30 to 260 °C with a constant heating rate of 10 °C/min.

2.5.5. Transmission electron microscopy (TEM)

The CNCs were analyzed under a transmission electron microscope (TEM Zeiss EM109B). The CNC suspension was sonicated for 30 min and was dropped on a nickel-Formvar©-coated 300-mesh grid for 2 min, and then drained on the filter paper. The grid was inverted and placed on top of a drop of 2% (w/v) uranyl acetate for 5 min. This process was repeated twice. After 24 h of drying in a cabinet at room temperature, the grids were viewed by TEM.

2.5.6. Zeta potential

A suspension of CNC was diluted (1:50 v/v) with distilled water and then filtered using a cellulose acetate/nitrate membrane with a porous diameter of 0.45 μm. Zeta potential was analyzed using 3000 NanoZS Zetasizer (Malvern).

2.5.7. Tensile testing of composite films

The films were cut into 1.5 cm wide × 15 cm long strips and were kept in a desiccator with $Mg(NO_3)_2$ at 23 °C and a relative humidity of 50% for 40 h. The assays were performed on a universal testing machine DL10000 (EMIC) in accordance with ASTM D882-12 (2012).

Table 1
Assignments of bands from FTIR spectra of banana pseudostem (Pacovan variety).

Wavenumber (cm^{-1})[a]	Assignment	Source
1726 (sh)	C=O stretching	Aliphatic carboxylic acid and ketones of hemicellulose
1635 (s)	OH bending/C=C stretching and ArC=O stretching	Water/Lignin
1515 (vw)	C=C aromatic skeletal vibration	Lignin
1324 (ms)	O—H in plane deformation	Cellulose
1254 (w)	C—O stretching/C=C stretching	Cellulose, Hemicellulose/Lignin
1056 (s), 1042 (s)	C—O stretching of COH and C—O—C symmetric stretching	Cellulose, Hemicellulose, Lignin
894 (vw)	C—H deformation	Cellulose, Hemicellulose
774 (vw)	ArC—H out of plane deformation	Lignin

Band intensity: s = strong; ms = medium strong; w = weak; vw = very weak; sh = shoulder.

[a] References: Bilba, Arsena, and Ouensanga (2007), Gañán, Cruz, Garbizu, Arbelaiz, and Mondragon (2004), Guimarães et al. (2009), Rosa et al. (2010), Socrates (2004).

2.5.8. Water vapor permeability (WVP)

The films were conditioned in a desiccator with $Mg(NO_3)_2$ at 25 °C and a relative humidity of 53% for 24 h. The WVP was determined using eight replicates at 24 °C and a relative humidity of 55%, using silica gel as the desiccant according to standard methods (ASTM E96-80, ASTM 1989).

2.5.9. Color and opacity

The films were analyzed four times at three different places along the films using a Hunter Lab System equipped with a chroma meter CR-300 (Konica Minolta). The color was measured as lightness (L^*), chroma (C^*), and hue (H^*) values (Azeredo, Miranda, Ribeiro, Rosa, & Nascimento, 2012).

The films were cut into 1 × 4 cm strips and were inserted into cuvettes with an optical length of 10 mm in a Cary 50 UV–Vis (Agilent) spectrophotometer. The transmittance of the films was measured by determining the absorbed energy at 400 and 800 nm (Savadekar & Mhaske, 2012).

3. Results and discussion

3.1. Chemical characterization

The BPF (Fig. 1a) presented a cellulose content (22.9 ± 1.2) two times higher than the hemicellulose content (11.3 ± 2.3), and almost three times higher than that of lignin (8.4 ± 1.9). The bleaching treatment eliminated the chromophoric contaminants in the BPF (Fig. 1b) and generated a brighter cellulose pulp. Other residual biomasses, as coconut husk (Rosa et al., 2010) or palm oil fiber (Fahma, Iwamoto, Hori, Iwata, & Takemura, 2010), demand a more laborious and reagent-intensive bleaching procedure, because of their high lignin content. By the other hand, BPF was successfully bleached with a relatively simple methodology.

3.2. FTIR characterization

The FTIR spectra of raw fibers, bleached fibers, and CNCs are shown in Fig. 1c, while Table 1 presents the corresponding peaks.

The peak at 1726 cm^{-1} is associated with carboxylic acids and aliphatic ketones present in hemicellulose. Their absence in the bleached fiber and in the CNC spectra is evidence for the removal of such components (Li, Wang, Li, Cheng, & Adhikari, 2014). The intensity of the peaks at 1254 cm^{-1} and 1042–1056 cm^{-1}, which are related to cellulose, hemicellulose, and lignin, decreased with the removal of a portion of the organic contents, probably in the form of hemicelluloses and lignin. The intensity of the peak at 894 cm^{-1}, which is attributed to cellulose and hemicellulose, increased as a function of the chemical treatments. The peak stretching from 1319–1326 cm^{-1} is related to cellulose O–H in-plane deformation (Socrates, 2004). The reduction of this peak in the CNC suggests the substitution of hydrogen by a sulfate group after acidic hydrolysis.

The peak stretching from 1631–1635 cm^{-1} is associated with adsorbed water (Abraham et al., 2011; Socrates, 2004) and the conjugated carbonyl group C=O of lignin (Du et al., 2010). This peak was evident in the raw fiber, and its intensity decreased in the bleached fiber, probably because of the removal of lignin. However, this peak remained in CNCs, probably owing to the presence of adsorbed water in the material. The intensity of the peaks at 1512–1515 and 774 cm^{-1}, which are related to lignin, decreased in the bleached fiber and were absent in the CNC spectra. This confirmed the successful removal of lignin in the CNCs after chemical treatments.

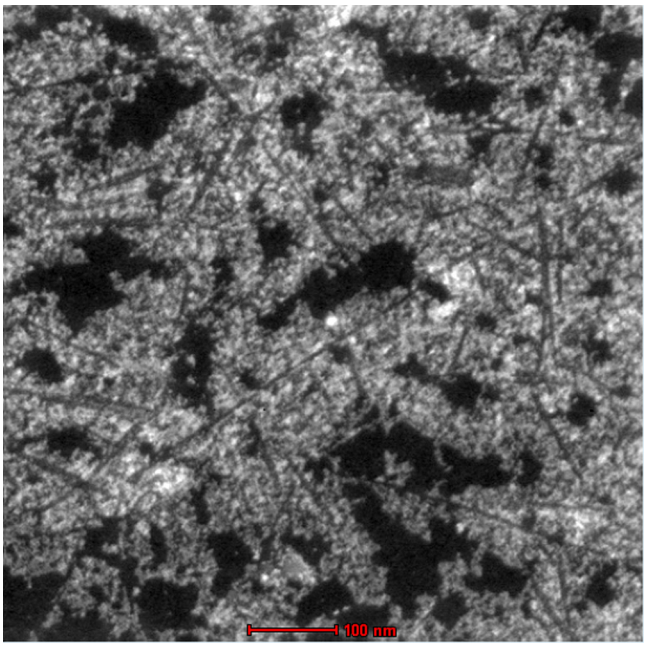

Fig. 2. TEM image of cellulose nanocrystals (CNCs) from banana pseudostem fiber (BPF).

3.3. TEM and zeta potential

The CNCs obtained from bleached BPF exhibit the typical characteristic clusters of well-defined needle-shaped particles (Fig. 2). According to the measurements, the mean length (L) of the nanostructures was 135.0 ± 12 nm, the mean diameter (D) was 7.2 ± 1.9 nm, and the mean aspect ratio (L/D) was 21.2 ± 2.8. These measurements were close to those of other reported CNCs (Cherian et al., 2008; Mueller et al., 2014).

Moreover, the CNCs from the bleached BPF have a higher aspect ratio than cotton nanofibers (Teixeira et al., 2010), sugarcane bagasse nanocellulose (Mandal & Chakrabarty, 2011), and ramie (Menezes, Siqueira, Curvelo, & Dufresne, 2009), but lower than coconut husk fiber (Rosa et al., 2010), corncob (Silvério, Flauzino Neto, & Pasquini, 2013), and sisal (Siqueira, Bras, & Dufresne, 2009). This intermediate aspect ratio may help in the further tailoring of cellulose nanocomposites.

Table 2
Mechanical and barrier properties of PVA film and PVA–nanocellulose composites.

Composite	Tensile strength (MPa)	Elongation at break (%)	Young' modulus (MPa)	WVP (g.mm/kPa.h.m^2)
PVA0	38.5 ± 3.6	61.0 ± 19.3	2522 ± 437	0.61 ± 0.04
PVA1	42.1 ± 1.2	96.1 ± 7.6	2570 ± 146	0.56 ± 0.03
PVA3	46.0 ± 2.7	74.3 ± 17.2	2940 ± 218	0.51 ± 0.03
PVA5	35.4 ± 0.5	83.0 ± 12.5	2586 ± 74	0.44 ± 0.01

The zeta potential of CNCs was −26.1 ± 3.7 mV. Modulus values higher than 25.0 mV result in stable colloidal suspensions (Mirhosseini, Tan, Hamid, & Yusof, 2008; Zhou et al., 2012). Teixeira et al. (2010) found a similar value for stable nanocellulose colloidal suspensions from brown cotton (ca. −26 ± 4 mV).

3.4. Tensile testing of composite films

The addition of CNCs from BPF improved the mechanical properties of the PVOH films up to 3% (Table 2). There was no major mechanical improvement in PVOH5. Roohani et al. (2008) and Zhou et al. (2012) reported the same trend in maximum stress and elastic modulus, which decreased as the CNC concentration increased.

The source of the cellulose nanocrystals may directly impact in the mechanical properties of the nanocomposite. Nanocomposites of PVOH with 3% of CNCs from cotton linter (aspect ratio (L/D) ≈12) yielded an increase of 19.4% in the tensile strength (Roohani et al., 2008); PVOH with 3% of nanofibers from microcrystalline cellulose ($L/D \approx 20$) showed an increase in the Young' modulus of 15.4% (Panaitescu et al., 2011), and PVOH with 3% of CNCs from corncob (L/D ≈ 53) presented a tensile strength of 30 MPa (Silvério et al., 2013), whilst the PVOH3, with CNCs from BPF ($L/D \approx 21$), presented respectively increments of 19.5%, 16.6%, and tensile strength of 46 MPa.

Uniform dispersions of CNCs are crucial for improving the mechanical properties of nanocomposites and for promoting the formation of hydrogen bonds between PVOH and CNCs. Uniform dispersion of the CNC leads to a more efficient transfer of stress between chains of the polymer matrix and the cellulose crystals (Liu, Sun, Tian, Maiti, & Ma, 2013; Zhou et al., 2012). For packaging applications, it is important to use a concentration of nanofiller that reinforces the maximum mechanical stress. So, the CNCs from BPF are suitable fillers to modify the neat PVOH film, resulting in an adequate nanocomposite for packaging.

3.5. Water vapor permeability (WVP)

The addition of CNCs decreased the WVP of the films (Table 2) by enlarging the path through the film that water molecules must pass by occupying the spaces between the molecules of the polymer matrix (Azeredo, Miranda, Ribeiro, et al., 2012; Azeredo, Miranda, Rosa, et al., 2012). The crescent concentration of CNCs presented a linear fitting with the decrease of WVP with $R^2 = 0.9886$.

Interactions between water and CNCs result in the rearrangements of water molecules in the matrix, lowering the plasticizing effect (Roohani et al., 2008) and increasing the barrier properties of the material. A decrease in WVP was reported previously for various nanocomposites such as alginate (Abdollahi, Alboofetileh, Behrooz, Rezaei, & Miraki, 2013), chitosan (Pereda, Dufresne, Aranguren, & Marcovich, 2014), polycaprolactone (Khan et al., 2013), and PVOH (Chen et al., 2012). Thus, the CNC is an important polymer to be added in the neat PVOH to allow the reduction in WVP.

3.6. Color and opacity

All the three colorimetric parameters presented a linear fit with the increase in the concentration of CNCs in the films (Fig. 3, Table 3). The lightness (L^*) ($R^2 = 0.9738$) decreased with the addition of CNCs, indicating the presence of some chromophoric substances (Fig. 3, Table 3). The higher the CNC concentration, the greater the change in the hue (H^*) ($R^2 = 0.9862$) toward yellow. Moreover, the chroma (C^*) ($R^2 = 0.9508$) also increased.

The crescent addition of CNCs in the PVOH films increased the amount of light absorbed by the films, increasing the opacity (Fig. 3,

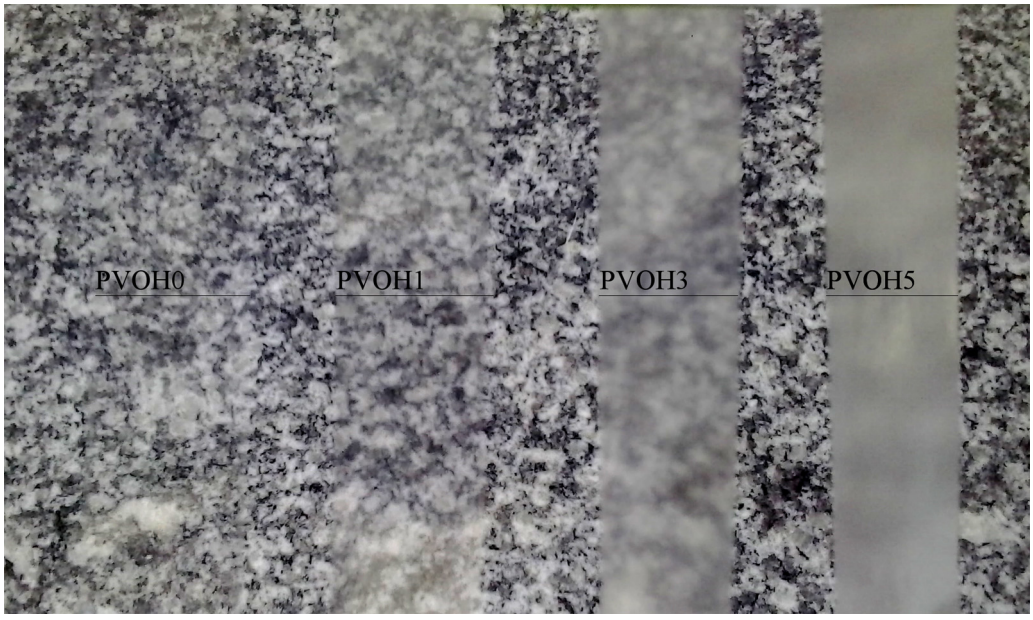

Fig. 3. PVA film and PVA-nanocellulose composites.

Table 3
Colorimetric and transmittance properties of PVA film and PVA-nanocellulose composites.

Composites	Lightness (L^*)	Chroma (C^*)	Hue (H°)	Transmittance at 600 nm (%)	Transmittance at 700 nm (%)
PVOH0	94.83 ± 0.06	2.57 ± 0.01	94.14 ± 0.20	88.47	88.93
PVOH1	94.70 ± 0.06	2.76 ± 0.01	93.47 ± 0.16	88.35	89.48
PVOH3	94.48 ± 0.05	3.31 ± 0.01	92.41 ± 0.24	86.85	87.99
PVOH5	94.05 ± 0.03	3.97 ± 0.01	91.24 ± 0.10	83.85	85.28

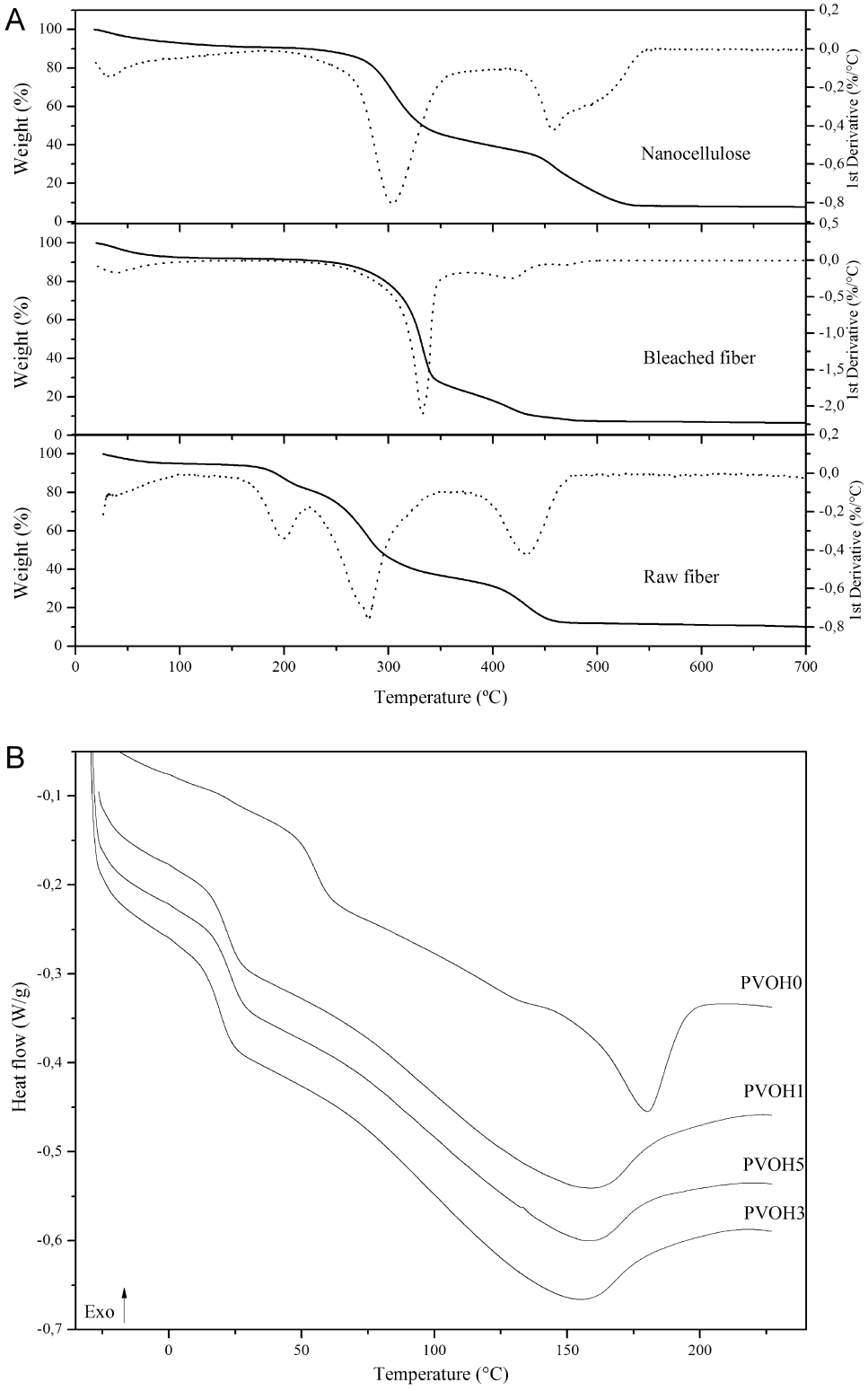

Fig. 4. (a) TGA (solid line) and dTG (dotted line) of raw banana pseudostem fiber (BPF) (bottom), bleached BPF (middle), and nanocellulose (top); (b) DSC of PVA film and PVA–nanocellulose composites.

Table 4
Thermal events, weight loss, and residues at 700 °C of raw banana fiber, bleached banana fiber, and extracted nanocellulose.

Events	T_{max} (°C)			Weight loss (%)		
	Raw fiber	Bleached. fiber	Nanocellulose	Raw fiber	Bleached. fiber	Nanocellulose
1°	36.1	37.2	30.9	5.1	8.3	9.4
2°	199	–	–	13.4	–	–
3°	280	333	303	45.5	68.3	52.9
4°	433	419	458	25.0	17.1	29.7
Residues at 700 °C				11.0	6.3	5.6

Table 3) as well, in a similar mechanism as that of the influence in the WVP. The CNC fills the voids between the chains of the polymer matrix, increasing the number of hurdles the light must pass through the material (Fortunati et al., 2013; Savadekar & Mhaske, 2012; Silvério et al., 2013). All casted films presented a transmittance as high as 80%; therefore, all the composites can be considered transparent (Bardet, Belgacem, & Bras, 2013; Wang, Yu, Zhang, He, & Zhang, 2013), indicating that the CNC addition did not affected the PVOH films in a way that could prevent the nanocomposite as a transparent material.

3.7. Thermal analyses (TGA and DSC)

The TG and dTG of the raw fiber, bleached fiber, and CNCs (Fig. 4a; Table 4) exhibited a thermal event around 100 °C, probably due to the loss of water, indicating increased hydrophilicity in the bleached BPF and CNCs.

The raw BPF presented four thermal events, while the bleached BPF and CNCs presented only three events. The absence of the second event in the bleached BPF, higher thermal stability in the bleached fiber, and shifting of the third event (cellulose pyrolysis) from 280 °C to 333 °C were due to the removal of hemicellulose and other easily degradable constituents by chemical treatments (Guimarães, Frollini, Silva, Wypych, & Satyanarayana, 2009). The reduction in the T_{max} of this peak from 333 °C in the bleached BPF to 303 °C in the nanocellulose must be caused by the sulfonation of the CNCs (Fahma et al., 2010; Fahma, Iwamoto, Hori, Iwata, & Takemura, 2011; Martins, Teixeira, Corrêa, Ferreira, & Mattoso, 2011; Teixeira et al., 2010, 2011).

Nanocellulose showed the highest T_{max} and mass loss in the fourth event, which was attributed to the oxidation and breakdown of carbonized residues to gaseous products with lower molecular masses. In the case of CNCs obtained by hydrolysis with H_2SO_4, this was attributed to the sulfate groups (Fahma et al., 2010; Neto, Silvério, Dantas, & Pasquini, 2013; Teixeira et al., 2010, 2011). The bleached fiber and nanocellulose presented lower-residue contents at 700 °C, indicating the removal of inorganic compounds by the chemical treatments. The nanocellulose from BPF showed a higher thermal stability in comparison to other CNCs, as from coconut husk (Rosa et al., 2010), white and colored cotton fibers (Teixeira et al., 2010), and soy hull (Flauzino Neto et al., 2013).

The DSC analysis (Fig. 4b) shows that the addition of nanocellulose reduced the thermal properties of the composites in the glass transition temperature (T_g), early melting point (T_{ONSET}), and maximum melting temperature (T_M). This was due to the hydrophilicity of the nanocellulose particles, which increased the amount of adsorbed water after drying the film. Moreover, water acted as a plasticizer (Roohani et al., 2008). This decrease was important because the melting temperature and the degradation temperature of PVOH are very close. Thus, this decrease enhanced the processing of the PVOH composites (Kuraray, 2014). Roohani et al. (2008) observed similar changes in PVOH films that were partially hydrolyzed with nanocellulose linter, what corroborates the fundamental role of the CNCs in the modification of this physical property of the nanocomposite, in comparison to the neat PVOH.

4. Conclusion

The BPF is a carbohydrate source suitable to obtain water-stable nanocellulose suspensions with good dimensions and better thermal stability than BPF raw fibers. The BPF nanocellulose, up to a concentration of 3%, improves the tensile strength, maximum stress modulus of elasticity, and barrier properties of the neat PVA films, but only slightly affects the color and brightness, without compromising the transparency of the films. This overall benefit of banana CNC in the PVOH films present an important application of BPF nanocellulose in packaging materials.

Acknowledgments

We thank Prof. José Marcos Sasaki, for the X-ray analyses, INCT-INOMAT and CNPq for the financial support, and CNPq and FUNCAP for the scholarship. We also thank Departamento de Química Orgânica e Inorgânica of Universidade Federal do Ceará for the FTIR analysis, Laboratório de Termoanálises do Departamento de Química Orgânica e Inorgânica da Universidade Federal do Ceará for the thermogravimetric analysis, Fundação Oswaldo Cruz, Centro de Pesquisa Aggeu Magalhães, for the METs and Abdulrazak B Ibrahim for help with the translation and review of the manuscript in English.

References

Abdollahi, M., Alboofetileh, M., Behrooz, R., Rezaei, M., & Miraki, R. (2013). Reducing water sensitivity of alginate bio-nanocomposite film using cellulose nanoparticles. *International Journal of Biological Macromolecules*, *54*, 166–173.
Abdul Khalil, H. P. S., Bhat, A. H., & Ireana Yusra, A. F. (2012). Green composites from sustainable cellulose nanofibrils: A review. *Carbohydrate Polymers*, *87*, 963–979.
Abraham, E., Deepa, B., Pothan, L. A., Jacob, M., Thomas, S., Cvelbar, U., et al. (2011). Extraction of nanocellulose fibrils from lignocellulosic fibres: A novel approach. *Carbohydrate Polymers*, *86*, 1468–1475.
ASTM–D882-12. (2012). *Standard test method for tensile properties of thin plastic sheeting.*
ASTM–E96-80. (1989). *Standard test methods for water vapor transmission of materials.*
Azeredo, H. M. C., Miranda, K. W. E., Ribeiro, H. L., Rosa, M. F., & Nascimento, D. M. (2012). Nanoreinforced alginate-acerola puree coatings on acerola fruits. *Journal of Food Engineering*, *113*, 505–510.
Azeredo, H. M. C., Miranda, K. W. E., Rosa, M. F., Nascimento, D. M., & Moura, M. R. (2012). Edible films from alginate-acerola puree reinforced with cellulose whiskers. *Food Science and Technology*, *46*, 294–297.
Azizi Samir, M. A. S., Alloin, F., & Dufresene, A. (2005). Review of recent research into cellulosic whiskers, their properties and their application in nanocomposite field. *Biomacromolecules*, *6*, 612–626.
Bardet, R., Belgacem, M. N., & Bras, J. (2013). Different strategies for obtaining high opacity films of MFC with TiO_2 pigments. *Cellulose*, *20*, 3025–3037.
Bilba, K., Arsena, M.-A., & Ouensanga, A. (2007). Study of banana and coconut fibers: Botanical composition, thermal degradation and textural observations. *Bioresource Technology*, *98*, 58–68.
Borysiak, S., & Doczekalsaka, B. (2005). X-ray diffraction study of pine wood treated with NaOH. *Fibres and Textiles in Easters Europe*, *13*, 87–89.
Chen, D., Lawton, D., Thompson, D. R., & Liu, Q. (2012). Biocomposites reinforced with cellulose nanocrystals derived from potato peel waste. *Carbohydrate Polymers*, *90*, 709–716.
Cherian, B. M., Pothan, L. A., Nguyen-Chung, T., Menning, G., Kottaisamy, M., & Thomas, S. (2008). A novel method for the synthesis of cellulose nanofibril whiskers from banana fibers and characterization. *Journal of Agricultural and Food Chemistry*, *56*, 5617–5627.

Du, H., Wang, W., Wang, Q., Zhang, Z., Sui, S., & Zhang, Y. (2010). Effects of pigments on the UV degradation of wood-flour/HDPE composites. *Journal of Applied Polymer Science*, *118*, 1068–1076.
Dufresne, A. (2012). *Nanocellulose: From nature to high performance tailored materials*. Berlin: Walter De Gruyter Incorporated.
Elanthikkal, S., Gopalakrishapanicker, U., Varghese, S., & Guthrie, J. T. (2010). Cellulose microfibres produced from banana plant wastes: Isolation and characterization. *Carbohydrate Polymers*, *80*, 852–859.
Fahma, F., Iwamoto, S., Hori, N., Iwata, T., & Takemura, A. (2010). Isolation, preparation, and characterization of nanofibers from oil palm empty-fruit-bunch (OPEFB). *Cellulose*, *17*, 977–985.
Fahma, F., Iwamoto, S., Hori, N., Iwata, T., & Takemura, A. (2011). Effect of pre-acid-hydrolysis treatment on morphology and properties of cellulose nanowhiskers from coconut husk. *Cellulose*, *18*, 443–450.
FAOStat. (2014). *FAOStat, Food and Agriculture Organization of the United Nations*. http://faostat.fao.org/site/567/default.aspx#ancor
Faruk, O., Bledzkia, A. K., Fink, H. P., & Sain, M. (2012). Biocomposites reinforced with natural fibers: 2000–2010. *Progress in Polymer Science*, *37*, 1152–1596.
Flauzino Neto, W. P., Silvério, H. A., Dantas, N. O., & Pasquini, D. (2013). Extraction and characterization of cellulose nanocrystals from agro-industrial residue – Soy hulls. *Industrial Crops and Products*, *42*, 480–488.
Fortunati, E., Puglia, D., Luzi, F., Santulli, C., Kenny, J. M., & Torre, L. (2013). Binary PVA bio-nanocomposites containing cellulose nanocrystals extracted from different natural sources: Part I. *Carbohydrate Polymers*, *97*, 825–836.
Frone, A. N., Panaitescu, D. N., Donescu, D., Spataru, C. I., Radovici, C., Truska, R., et al. (2011). Preparation and characterization of PVOH composites with cellulose nanofibers obtained by ultrasonication. *Bioresources*, *6*, 487–512.
Gañán, P., Cruz, J., Garbizu, S., Arbelaiz, A., & Mondragon, A. (2004). Stem and bunch banana fibers from cultivation wastes: Effect of treatments on physico-chemical behavior. *Journal of Applied Polymer Science*, *94*, 1489–1495.
Guimarães, J. L., Frollini, E., Silva, C. G., Wypych, F., & Satyanarayana, K. G. (2009). Characterization of banana, sugarcane bagasse and sponge gourd fibers of Brazil. *Industrial Crop and Products*, *30*, 407–415.
Jiang, B., Liu, C., Zhang, C., Wang, B., & Wang, Z. (2007). The effect of non-symmetric distribution of fiber orientation and aspect ratio on elastic properties of composites. *Composites Part B: Engineering*, *38*, 24–34.
Khan, R. A., Beck, S., Dussault, D., Salmieri, S., Bouchard, J., & Lacroix, M. (2013). Mechanical and barrier properties of nanocrystalline cellulose reinforced poly(caporlactone) composites: Effect of gamma radiation. *Journal of Applied Polymer Science*, *129*, 3038–3046.
Khider, T. O., Omer, S. H., & Elzaki, O. T. (2012). Pulping and totally chlorine free (TCF) bleaching of *Acacia mellifera* from Sudan. *World Applied Sciences Journal*, *16*, 1256–1261.
Kuraray. ®Mowiol Technical data sheet, 2010. http://www.kuraray.eu/fileadmin/Downloads/mowiol/TDS_Mowiol_16012014.pdf Accessed 19.01.14.
Kvien, I., & Oksman, K. (2007). Orientation of cellulose nanowhiskers in polyvinyl alcohol (PVA). *Applied Physics A*, *87*, 641–643.
Li, M., Wang, L.-J., Li, D., Cheng, Y.-L., & Adhikari, B. (2014). Preparation and characterization of cellulose nanofibers from de-pectinated sugar beet pulp. *Carbohydrate Polymers*, *102*, 136–143.
Liu, D., Sun, X., Tian, H., Maiti, S., & Ma, Z. (2013). Effects of cellulose nanofibrils on the structure and properties on PVA nanocomposites. *Cellulose*, *20*, 2981–2989.
Mandal, A., & Chakrabarty, D. (2011). Isolation of nanocellulose from waste sugarcane bagasse (SCB) and its characterization. *Carbohydrate Polymers*, *86*, 1291–1299.
Martins, M. A., Teixeira, E. M., Corrêa, A. C., Ferreira, M., & Mattoso, L. H. C. (2011). Extraction and characterization of cellulose whiskers from commercial cotton fibers. *Journal of Materials Science*, *46*, 7858–7864.
Menezes, A. J., Siqueira, G., Curvelo, A. A. S., & Dufresne, A. (2009). Extrusion and characterization of functionalized cellulose whiskers reinforced polyethylene nanocomposite. *Polymer*, *50*, 4552–4563.
Mirhosseini, H., Tan, C. P., Hamid, N. S. A., & Yusof, S. (2008). Effect of arabic gum, xanthan gum and orange oil contents on zeta-potential, conductivity, stability, size index and pH of orange beverage emulsion. *Colloids and Surfaces A: Physicochemical and Engineering Aspects*, *315*, 47–56.
Moon, R. J., Martini, A., Nairn, J., Simonsen, J., & Youngblood, J. (2011). Cellulose nanomaterials review: Structure, properties and nanocomposites. *Chemical Society Reviews*, *40*, 3941–3994.
Mueller, S., Weder, C., & Foster, E. J. (2014). Isolation of cellulose nanocrystals from pseudostems of banana plants. *RSC Advances*, *4*, 907–915.
Orts, W. J., Shey, J., Imam, S. H., Glenn, G. M., Guttman, M. E., & Revol, J. F. (2005). Application of cellulose microfibrils in polymer nanocomposites. *Journal of Polymers and Environment*, *13*, 301–306.
Padam, B. S., Tin, H. S., Chye, F. Y., & Abdullah, M. I. (2012). Banana by-products: An under-utilized renewable food biomass with great potential. *Journal of Food Science and Technology*, *49*, 1–19.
Panaitescu, D. M., Frone, A. N., Ghiurea, M., Spataru, C. I., Radovici, C., & Iorga, M. D. (2011). Properties of polymer composites with cellulose microfibrils. In B. Attaf (Ed.), *Advances in composites materials – Ecodesign and analysis* (pp. 103–122). Rijeka: InTech Europe.
Pereda, M., Dufresne, A., Aranguren, M. I., & Marcovich, N. E. (2014). Polyelectrolyte films based on chitosan/olive oil and reinforced with celulose nanocrystals. *Carbohydrate Polymers*, *101*, 1018–1026.
Rescignano, N., Fortunati, E., Montesano, S., Emiliani, C., Kenny, J. M., Martino, S., et al. (2014). PVA bio-nanocomposites: A new take-off using celulose nanocrystals and PLGA nanoparticles. *Carbohydrate Polymers*, *99*, 47–58.
Roohani, M., Habibi, Y., Belgassem, N. M., Ebrahim, G., Karimi, A. N., & Dufresne, A. (2008). Cellulose whiskers reinforced polyvinyl alcohol copolymers nanocomposites. *European Polymer Journal*, *44*, 2489–2498.
Rosa, M. F., Medeiros, E. S., Malmonge, J. A., Gregorski, K. S., Wood, D. F., Mattoso, L. H. C., et al., & Orts, W. J. (2010). Cellulose nanowhiskers from coconut husk fibers: Effect of preparation conditions on their thermal and morphological behavior. *Carbohydrate Polymers*, *81*, 83–92.
Rosa, S. M. L., Rehman, N., Miranda, M. I. G., Nachtigall, S. M. B., & Bica, C. I. D. (2012). Chlorine-free extraction of cellulose from rice husk and whisker isolation. *Carbohydrate Polymers*, *87*, 1131–1138.
Santa-Maria, M., Ruiz-Colorado, A. A., Cruz, G., & Jeoh, T. (2013). Assessing the feasibility of biofuel production from lignocellulosic banana waste in rural agricultural communities in Peru and Colombia. *BioEnergy Research*, *6*, 1000–1011.
Savadekar, N. R., & Mhaske, S. T. (2012). Synthesis of nano cellulose fibers and effect on thermoplastics starch based films. *Carbohydrate Polymers*, *89*, 146–151.
Silvério, H. A., Flauzino Neto, W. P., & Pasquini, D. (2013). Effect of incorporating cellulose nanocrystals from corncob on the tensile, thermal and barrier properties of poly(vinyl alcohol) nanocomposites. *Journal of Nanomaterials*, *2013*, 1–9.
Siqueira, G., Bras, J., & Dufresne, A. (2009). Cellulose whiskers versus microfibrils: Influence of the nature of the nanoparticle and its surface functionalization on the thermal and mechanical properties of nanocomposites. *Biomacromolecules*, *10*, 425–432.
Socrates, G. (2004). *Infrared and Raman characteristic group frequencies: Tables and charts* (3rd ed.). New York: John Willey & Sons.
TAPPI. (1997). *T 204 om-97. Solvent extractives of wood and pulp*.
TAPPI. (2000). *T 222 om-02. Acid-insoluble lignin in wood and pulp*.
TAPPI. (2002). *T 421 om-02. Moisture in pulp, paper and paperboard*.
TAPPI. (2009). *T 203 cm-99. Alpha-, beta- and gamma-cellulose in pulp*.
Teixeira, E. M., Corrêa, A. C., Manzoli, A., Leite, F. L., De Oliveira, C. R., & Mattoso, L. H. C. (2010). Cellulose nanofibers from white and naturally colored cotton fibers. *Cellulose*, *17*, 595–606.
Teixeira, E. M., Bondancia, T. J., Teodoro, K. B. R., Corrêa, A. C., Marconcini, J. M., & Mattoso, L. H. C. (2011). Sugarcane bagasse whiskers: Extraction and characterizations. *Industrial Crops and Products*, *33*, 63–66.
Tingaut, P., Zimmermann, T., & Sèbe, G. (2012). Cellulose nanocrystals and microfibrillated cellulose as building blocks for the design of hierarchical functional materials. *Journal of Materials Chemistry*, *22*, 20105–20111.
Wang, D., Yu, J., Zhang, J., He, J., & Zhang, J. (2013). Transparent bionanocomposites with improved properties from poly(propylene carbonate) (PPC) and cellulose nanowhiskers (CNWs). *Compostes Science and Technology*, *85*, 83–89.
Yokoyama, T., Kadla, J. F., & Chang, H.-M. (2002). Microanalytical method for the characterization of fiber components and morphology of woody plants. *Journal of Agriculture and Food Chemistry*, *50*, 1040–1044.
Yousefi, H., Faezipour, M., Hedjazi, S., Mousavi, M. M., Azusa, Y., & Heidari, A. H. (2013). Comparative study of paper and nanopaper properties prepared from bacterial cellulose nanofibers and fibers/ground cellulose nanofibers of canola straw. *Industrial Crops and Products*, *43*, 732–737.
Zhou, Y. M., Fu, S. Y., Zheng, L. M., & Zhan, H. Y. (2012). Effect of nanocellulose isolation techniques on the formation of reinforced poly(vinyl alcohol) nanocomposite films. *Express Polymer Letters*, *6*, 794–804.